Optic Disc Localization in Retinal Images

Florin Rotaru, Silviu Ioan Bejinariu, Cristina Diana Niță, and Mihaela Costin

Institute of Computer Science, Romanian Academy, Iasi Branch, Romania
{florin.rotaru,silviu.bejinariu,cristina.nita,
mihaela.costin}@iit.academiaromana-is.ro

Abstract. The paper proposes an optic disc localisation method in color retinal images. It is a first step of a retinal image analysis project which will be completed later with other tasks as fovea detection and measurement of retinal vessels. The final goal is to detect in early stages signs of ophthalmic pathologies as diabetic retinopathy or glaucoma, by successive analysis of ophthalmoscopy images. The proposed method first detects in the green component of RGB image the optic disc area and then on the segmented area extracts the optic disc edges and obtains a circular optic disc boundary approximation by a Hough transform.

Keywords: optic disc, retinal images, vessel segmentation, Hough transforms.

1 Introduction

The traditional assessment way of ophthalmic pathologies signs is prone to the presence of specially trained examiners. More than that sophisticated measurements on the fundus images are not possible by direct visualization. Since the early detection of these diseases is crucial for a reasonable treatment and the traditional ways do not cope with this complex task, automatic analysis is required to assist the specialists. Even in the last decade many automatic methods were proposed the problem is not yet fully solved, mainly due to the large variations between individuals and uneven quality and diversity of the acquired retinal images.

However, some important results were achieved. Part of the proposed techniques, so called bottom-up methods, first locates the optic disc and then starting from that area track the retinal vessels and do the required measurements. The analysis of optic disc area is essential for diagnosis of different aspects caused by diabetic retinopathy. Also, optic disc segmentation can be useful for detection of some other eye condition as glaucoma, which can be diagnosed by identifying the changes in the optic disc area. Another important argument for optic disc recognition is that once the disc is located, the fovea localization, otherwise difficult to compute, becomes an easier task due the relatively constant distance between the fovea and optic disc.

A second group of techniques, top-down approaches, first track the retinal vessels and get the optic disc as the root of the vessels tree. There are arguments pro and contra for one or another approach. The presence of exudates makes very difficult the optic disc direct segmentation. In some other circumstances, as in the case of

V.E. Balas et al. (Eds.): Soft Computing Applications, AISC 195, pp. 453–463.
springerlink.com

peripapillary atrophy, bright areas in the very vicinity of the optic disc might distort its round shape. In these circumstances the direct localization of the disc becomes a quite challenging task. On the other hand vessels tracking might be a very difficult task if there are discontinuities in the vessel structure. We mention just two top-down approaches, [4] and [5]. While in [4] the retinal vessels convergence point is detected by employing a voting-type algorithm named fuzzy convergence, in [5] first there are identified the four main vessels in the image. Then the four branches are modeled by two parabolas whose common vertex is identified as optic disc centre.

A very known now bottom-up technique was proposed in [3]. The optic disc area localization is performed by employing a principal component analysis method. This implies a previous training step. Then a modified active shape model is proposed to identify the disc boundary.

Another important work is the one presented in [1]. Part of this methodology was also implemented in our system to process retinal images. First the optic disc area is located using a voting procedure. There were implemented three methods for a rough identification of optic disc area. The green channel of the RGB input image is used. The first method starts by filtering the green image using a 21 x 21 median filter. For each pixel in the filtered image is computed the difference between the maximum and minimum grey levels in a 21x21 window centered on the current pixel. As optic centre is chosen the pixel with the maximum difference. Second approach to approximate optic disc detection calculates the statistical variance for every pixel using a 71x71 window. Also, applying the Otsu technique the blue channel image is binarized. The pixel presenting the maximum statistical variance and having at least 10 white pixels in a 101x101 area centered on it but in the blue binarized channel is declared disc centre. Finally, the third voting method applies a Fourier transform to the input image. A Gaussian low-pass filter is applied in the frequency domain and the result image is transformed back in the spatial domain. The brightest pixel in the new image is taken as the third optic disc centre candidate. The voting procedure establishes the estimated disc centre in the following way: 1) if all three candidates are close to their centre this one is proposed as an approximate disc centre; 2) if only two from three candidates are close to the centre the average point of these two is chosen; 3) if all candidates are far apart from their centre the candidate proposed by the second method, the most reliable considered by the authors, is chosen.

Then a 400x400 window is centered on the estimated disc centre, and extracted from original green and red channels. A morphological filter is employed from [6] to erase the vessels in the new window. A Prewitt edge detector is then applied and by the same Otsu technique the image is binarised. The result is cleaned by morphological erosion and finally a Hough transform is applied to get the final optic disc boundary. Finally, the boundary with the best fitting from the two channels is chosen. The authors report for 1200 retinal images a score of 100% for approximated localisation and a score of 86% for final optic disc localization.

A mixed approached, independently detecting the optic disc centre and retinal vessels, is proposed in [2]. The vessels are segmented in the green channel of RGB retinal image using several image processing techniques. A first pre-processing step to smooth the homogenous regions of image without blurring vessel boundaries is done

applying a contrast limited adaptive histogram equalization followed by an edge-preserving anisotropic diffusion filter. Then the blood vessels are segmented using in a first stage a filtering technique based on eigenvalue analysis of the Hessian matrix. The result image is binarized by an iterative thresholding method. A skeletonization is applied on the vessel network. After processing the skeleton image to eliminate spurious branches, the vessel medians are superimposed on the original image. Starting from specific median points measurements of the vessel width are performed. Independently, several Mean Shift processes are equidistantly seeded in the green channel image. Using a circular kernel each process migrates to a local grey intensity maximum. The processes reaching low intensity values are disregarded and the centre with the maximum dark pixels around is chosen. To estimate the disc boundary the method proposed in [7] is then applied.

2 Optic Disc Recognition

In order to exactly locate the optic disc first we started following a similar methodology as the one proposed in [1]. Tests were done on 720x576 RGB retinal images, some of them of patients strongly affected by eye disorder. From the three methods of the voting procedure presented in [1] good optic disc area localization we obtained only with the Low-Pass Filter Method, the third method of the voting procedure in [1]. Our implementation it is a common one: to smooth out the little white patches which can perturb the right disc localization the green channel of the input image is transformed in frequency domain. As in [1] on the image of the magnitude of the FFT transform a Gaussian low-pass filter was applied:

$$H(u,v) = \exp\left(-\frac{D^2(u,v)}{2D_0^2}\right) \tag{1}$$

where $D(u,v)$ is the Euclidean distance from point (u,v) to the origin of frequency domain and D_0 is the cutoff frequency, of 25 Hz. The filtered result is transformed back to the spatial domain and the brightest pixel of the result image is chosen as an optic disc area centre candidate.

Good results were obtained also with another approach derived from the Maximum Difference Method proposed in [1]. As in [1] a 21x21 median filter is first applied on the green channel of the input image to eliminate isolated peaks. Then for each (i, j) pixel of the filtered green channel I (x, y) is calculated the difference between the maximum gray value and minimum gray value of the pixels inside a 21 x 21 window centered on the current (i, j) pixel:

$$Diff(i,j) = I_W^{max}(i,j) - I_W^{min}(i,j) \tag{2}$$

There are retained four pixels with the greatest values $Diff\ (i, j)$. Then, starting from texture operators:

$$\begin{aligned} L5 &= \begin{bmatrix} 1 & 4 & 6 & 4 & 1 \end{bmatrix} \\ E5 &= \begin{bmatrix} -1 & -2 & 0 & 2 & 1 \end{bmatrix} \\ S5 &= \begin{bmatrix} -1 & 0 & 2 & 0 & -1 \end{bmatrix} \end{aligned} \tag{3}$$

where:

L5 - mask to asses the gray level average;
E5 - edge mask;
S5 - corner mask.

the following masks, as in [8], are synthesized:

$$\begin{aligned} L5^{t}xE5 &= \begin{bmatrix} -1 & -2 & 0 & 2 & 1 \\ -4 & -8 & 0 & 8 & 4 \\ -6 & -12 & 0 & 12 & 6 \\ -4 & -8 & 0 & 8 & 4 \\ -1 & -2 & 0 & 2 & 1 \end{bmatrix} \quad L5^{t}xS5 = \begin{bmatrix} -1 & 0 & 2 & 0 & 1 \\ -4 & 0 & 8 & 0 & 4 \\ -6 & 0 & 12 & 0 & 6 \\ -4 & 0 & 8 & 0 & 4 \\ -1 & 0 & 2 & 0 & 1 \end{bmatrix} \\ E5^{t}xL5 &= \begin{bmatrix} -1 & -4 & -6 & -4 & -1 \\ -2 & -8 & -12 & -8 & -2 \\ 0 & 0 & 0 & 0 & 0 \\ 2 & 8 & 12 & 8 & 2 \\ 1 & 4 & 6 & 4 & 1 \end{bmatrix} \quad S5^{t}xL5 = \begin{bmatrix} -1 & -4 & -6 & -4 & -1 \\ 0 & 0 & 0 & 0 & 0 \\ 2 & 8 & 12 & 8 & 2 \\ 0 & 0 & 0 & 0 & 0 \\ -1 & -4 & -6 & -4 & -1 \end{bmatrix} \end{aligned} \tag{4}$$

For each pixel of the filtered green channel I(x,y) the texture parameter $f(i,j)$ is computed:

$$f(i,j) = \sqrt{(f_{L5^{t}xE5}(i,j))^2 + (f_{L5^{t}xS5}(i,j))^2 + (f_{E5^{t}xL5}(i,j))^2 + (f_{S5^{t}xL5}(i,j))^2} \tag{5}$$

The value $f(i,j)$ is normalized:

$$F(i,j) = \frac{f(i,j) - f_{\min}}{f_{\max} - f_{miin}} \tag{6}$$

where $f_{\max} = \max\{f(i,j)\}, f_{\min} = \min\{f(i,j)\}, 0 \le i \le H-1, \ 0 \le j \le W-1$. H is the image height and W is the image width.

From the four pixels with the greatest values $Diff(i,j)$ selected in the first stage is retained the one with the largest average of $F(i,j)$ computed on the 21x21 window centered on the processed pixel.

From our tests we conclude that on the retinal images of healthy patients or in the early stages of affection this second voting method provides a closer point to the real optic disc centre than the first one. However, on the retinal images strongly affected it fails. Finally, if the two methods to approximate the optic disc centre provide close centers is chosen the one computed by the second method. Otherwise the centre

computed by the first method is chosen. The results obtained with the two procedures are illustrated by figure 1, where the little cross is the point found out by maximum difference method and the big cross is the point provided by the second algorithm.

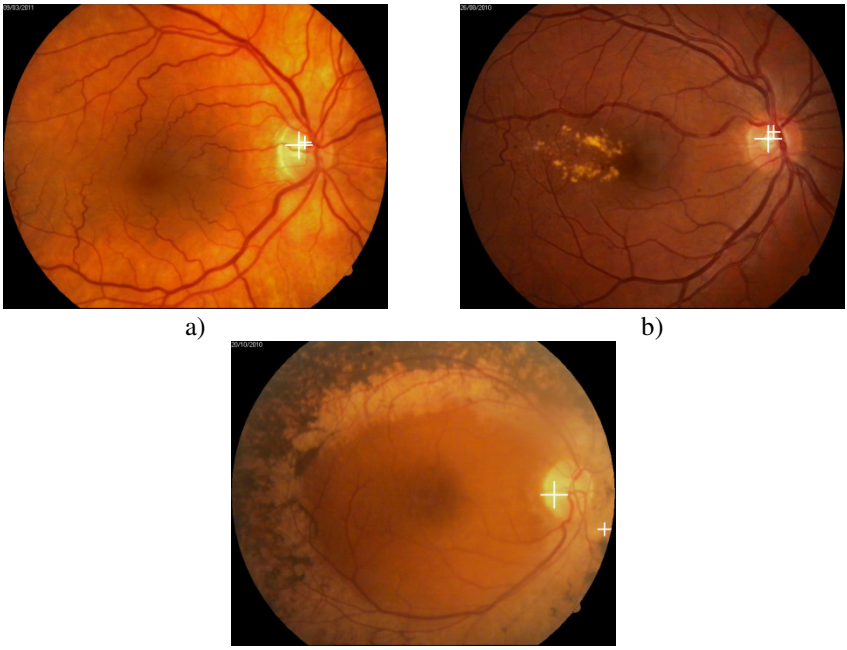

Fig. 1. Results of detecting approximate optic centre position by two voting procedures. Point marked with little cross is provided by the first method and the one indicated by large cross is computed by second voting algorithm. When the two points are far apart, as in the c) image, the centre computed by the first method is chosen.

Once the preliminary optic disc centre is established by voting procedure, as in [1], the further work was done on a window, 300x300 in our case, centered on the optic centre. The tests were done on green channel of 86retinal images. Following the same technique employed from [6] in the established window the blood vessels were eliminated. Next we shall describe shortly this method. The grayscale erosion on a image I by a structuring element B, as in [6], is the minimum grey value of the pixels in the vicinity defined by structuring element and centered on pixel (x,y):

$$[\varepsilon_B(I)](x,y) = \min_{(a,b)\in B} I(x+a, y+b) \tag{7}$$

For the same structuring element B the dilation is defined as the maximum grey value of the pixels:

$$[\delta_B(I)](x,y) = \min_{(a,b)\in B} I(x+a, y+b) \tag{8}$$

The opening $\gamma_B(I)$ of an image I by the structuring element B is:

$$\gamma_B(I) = \delta_B(\varepsilon_B(I)) \tag{9}$$

The closing $\varphi_B(I)$ of an image I by the structuring element B is:

$$\varphi_B(I) = \varepsilon_B(\delta_B(I)) \tag{10}$$

Considering as in [1] a line of 27 pixels length and 1 pixel width as the structuring element, for each of 12 different orientation of the line was performed an opening of the original 300x300 selected window. Noting the current image (300x300 window) with I , the clean image, without vessels, is:

$$I_B = \min_{i=1,\ldots 12}\left(\gamma_{B_i}(I)\right) \tag{11}$$

This means that each pixel of the result image has the minimum value from the set of 12 values of the same coordinate pixel in each of the 12 openings of I .

Results of the vessels erasing operation are illustrated by figure 2.

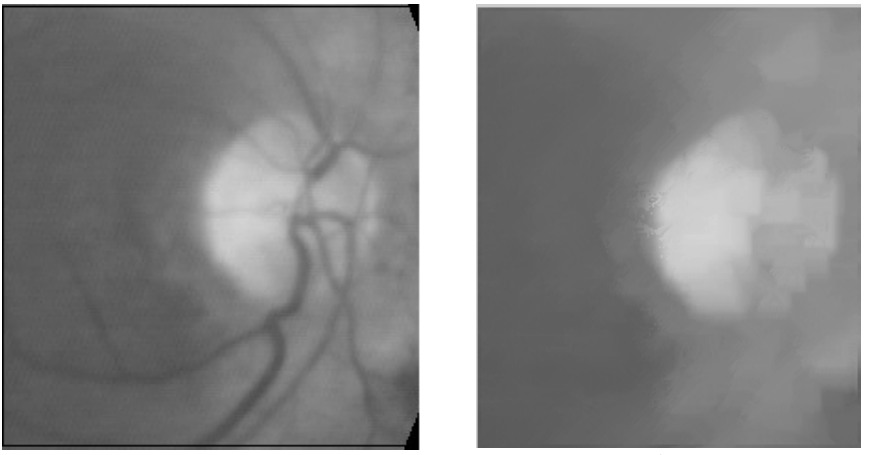

a) b)

Fig. 2. a) The 300x300 working window of image 1.c, also illustrated by figure 3.a. b) The result of vessels erasing

Tests have been made with different lengths of structuring element but no smoother images were obtained.

Eventually for further development, to measure the vessels width in certain point of interest, similar vessels segmentation technique as the one proposed in [6] will be tested. For instance in [6] from the initial image is obtained, in a similar way as image I_B , a cleaner image than the original one: $I_C = \max_{i=1,\ldots 12}\left(\gamma_{B_i}(I)\right)$. If the image I is used as a mask image and the image I_C as a marker image applying a reconstruction,

as defined in [6], a much cleaner image I_D is obtained: $I_D = R_I(I_C)$. The image with very clear segments of the vessels, suitable for measurements, is: $I_V = I_D - I_B$.

Coming back to our disc segmentation approach the next operation on image I_B is a Canny filtering followed by binarization to obtain the disc edges, in order to perform a final circle fitting. Let us note with I_{Canny} the binary image containing the Canny edges.

Due the great variability of pathology and image primary sources a fixed threshold for Canny filter is not desirable. We propose an iterative approach:

1. Compute a binarization threshold using Otsu method, [9], on image I_B, without performing the binarization.
2. Choose a value close to Otsu threshold as a primary threshold for Canny filtering.
3. Perform Canny filtering.
4. For an interval $[r_{\min}, r_{\max}]$ of circle radius compute a circle fitting by Hough transform applied on the whole window.
5. Choose the centre radius with the best fitting score and best distribution of fitting points.
6. If the fitting score is not desirable or there are few points to perform the fitting decrease the Canny threshold by a certain amount (constant in our implementation). Not more than a predefined number of iterations resume the process from step 3.
7. Even the fitting score and the distribution fitting points are acceptable run at least one more time all the cycle (steps 3-5) with a new Canny decreased threshold.
8. If the detected circles have comparable fitting scores and fitting point distributions choose the circle with the longest radius.

Results of the proposed approach are illustrated by figure 3 where are depicted: a) the original image from figure 1.c; b) the Canny edge extraction results for the starting threshold; c) Canny edges for adapted threshold; d) final circle.

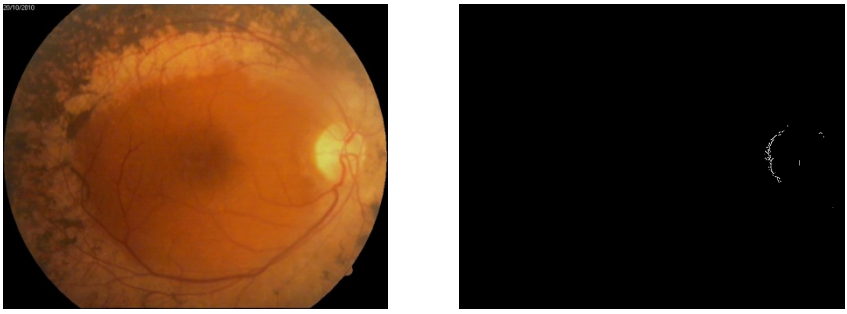

a) b)

Fig. 3. a) the input RGB image, in this case the same as in figure 1.c; b) the Canny edge extraction results for the starting threshold; c) Canny edges for adapted threshold; d) final circle.

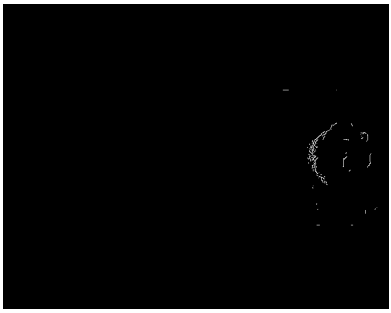

c)

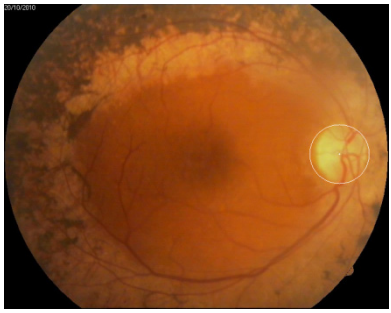

d)

Fig. 3. (*continued*)

While Canny filtering was performed using the OpenCV function for Hough transform we implemented our own method:

1 Create image accumulator I_{acc}.

2 For each radius integer r in the interval $[r_{\min}, r_{\max}]$ do:

2.1 Clean I_{acc}.

2.2 For each pixel $p(x_c, y_c)$ of I_{Canny} image do:

2.2.1 For $x = x_c - \frac{r}{2}$ to $x_c + \frac{r}{2}$ do:

2.2.1.1 $y_{frac} = \sqrt{r^2 - (r-x)^2}$

2.2.1.2 If there are pixels "1" in a 3x3 neighborhood of $I_{Canny}(x, y_c + y_{frac})$

then $I_{acc}(x_c, y_c) = I_{acc}(x_c, y_c) + 1$

2.2.1.3 If there are pixels "1" in a 3x3 neighborhood of $I_{Canny}(x, y_c - y_{frac})$

then $I_{acc}(x_c, y_c) = I_{acc}(x_c, y_c) + 1$

2.2.2 For $y = y_c - \frac{r}{2}$ to $y_c + \frac{r}{2}$ do:

2.2.2.1 $x_{frac} = \sqrt{r^2 - (r-y)^2}$

2.2.2.2 If there are pixels "1" in a 3x3 neighborhood of $I_{Canny}(x + x_{frac}, y)$

then $I_{acc}(x_c, y_c) = I_{acc}(x_c, y_c) + 1$

2.2.2.3 If there are pixels "1" in a 3x3 neighborhood of $I_{Canny}(x - x_{frac}, y)$

then $I_{acc}(x_c, y_c) = I_{acc}(x_c, y_c) + 1$

2.3 Choose the current centre the pixel $p(x_c, y_c)$ for which $I_{acc}(x_c, y_c) = \max_{x=1,n;\, y=1,m} I_{acc}(x, y)$.

2.4 Keep track of the best fitting circle considering the number of fitting points and the distance between the current circle centre and the mass centre of the fitting points.

We opted for our own Hough transform implementation in order to get more control on the distribution of the fitting points. This way some configurations can be rejected even there are generated by an acceptable number of fitting points if the points are not equally distributed around circle center.

3 Results and Conclusions

Tests have been done on 86 RGB retinal images of 720x576 resolution. The rough optic disc localization has been successful on whole the image set. The final circle fitting failed on two images strongly affected. Figure 4 illustrates some final circle localization results. The further tests will be done to validate and eventually to improve our optic disc detection approach.

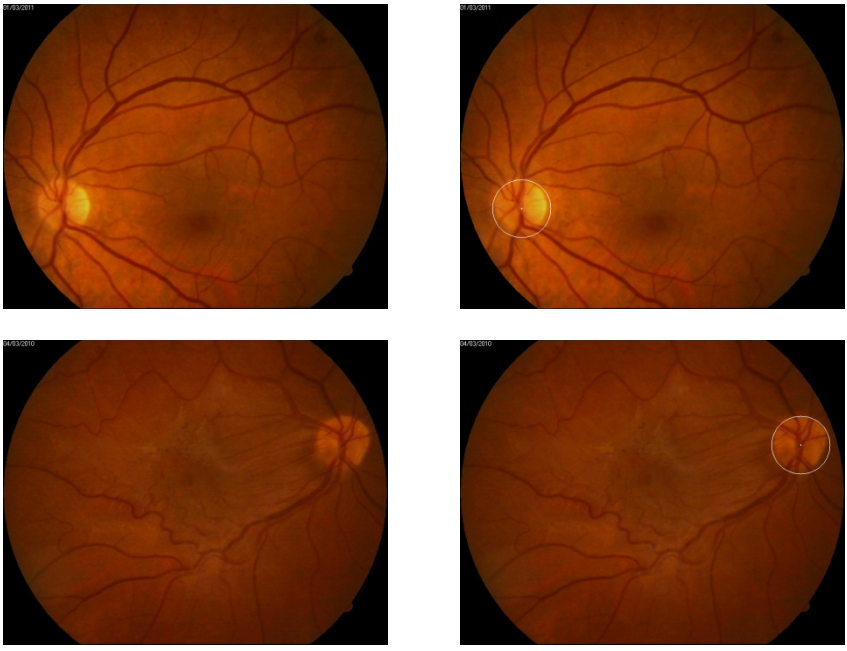

Fig. 4. On the left column: original retinal images. On the right: the final optic disc localization results.

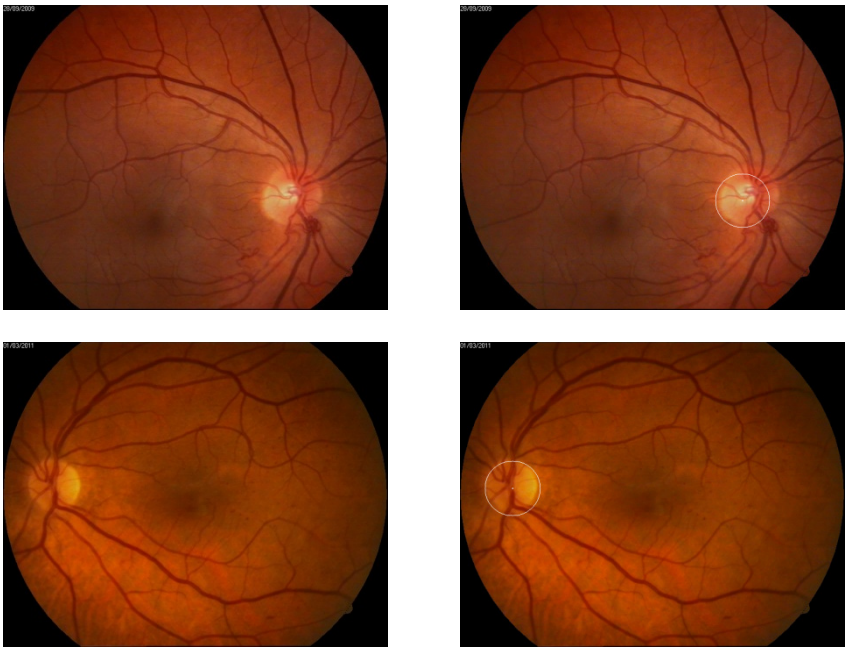

Fig. 4. (*continued*)

The reported work is a first stage of a larger project that will be completed later on with other tasks as fovea detection and measurement of retinal vessels. The final goal is to detect in early stages signs of ophthalmic pathologies as diabetic retinopathy or glaucoma.

The optic disk localization procedure was implemented and tested in an image processing framework developed by authors. It is implemented as a Windows application, in C++ using Microsoft Visual Studio. For image manipulation and some processing functions, the OpenCV library is used.

Acknowledgments. The work was done as part of a research contract with University of Medicine and Pharmacy „Gr.Popa" Iasi to analyze retinal images for early prevention of ophthalmic diseases. The authors would like to tank Dr. Traian Mihaescu for his assistance.

References

1. Aquino, A., Gegundez-Arias, M.E., Marin, D.: Detecting the Optic Disc Boundary in Digital Fundus Images Using Morphological, Edge Detection, and Feature Extraction Techniques. IEEE Transactions on Medical Imaging 29(11), 1860–(1869)
2. Manikis, G.C., Sakkalis, V., Zabulis, X., Karamaounas, P., Triantafyllow, A., Douma, S., Zamboulis, C., Marias, K.: An Image Analysis Framework for the Early Assesement of Hypertensive Retinopathy Signs. In: Proceedings of the 3rd IEEE International Conference on E-Health and Bioengineering - EHB 2011, Iaşi, Romania, November 24-26, pp. 413–418 (2011)

3. Li, H., Chutatape, O.: Automated Feature Extraction in Color Retinal Images by a Model Based Approach. IEEE Transactions on Biomedical Engineering 51(2), 246–254 (2004)
4. Hoover, A., Goldbaum, M.: Locating the optic nerve in a retinal image using the fuzzy convergence of the blood vessels. IEEE Trans. Med. Imag. 22(8), 951–958 (2003)
5. Foracchia, M., Grisan, E., Ruggeri, A.: Detection of optic disc in retinal images by means of a geometrical model of vessel structure. IEEE Trans. Med. Imag. 23(10), 1189–1195 (2004)
6. Heneghan, C., Flynn, J., O'Keefe, M., Cahill, M.: Characterization of changes in blood vessel width and tortuosity in retinopathy of prematurity using image analysis. Med. Image Anal. 6, 407–429 (2002)
7. Lindeberg, T.: Detecting salient blob-like image structures and their scales with a scale-space primal sketch: A method for focus-of attention. International Journal of Computer Vision 11, 283–318 (1993)
8. Guo, Y.: Computer-Aided Detection of Breast Cancer Using Ultrasound Images. PhD Thesis, Utah State University (2010)
9. Otsu, N.: A Threshold Selection Method from Gray-Level Histograms. IEEE Transactions on Systems, Man, and Cybernetics 9(1), 62–66 (1979)